Drug Design, Development and Therapy

Dovepress

open access to scientific and medical research

Open Access Full Text Article

ORIGINAL RESEARCH

A Novel Delivery System of RGD-HSA Loaded GEM/CUR Nanoparticles for the Treatment of Pancreatic Cancer Therapy

Tao Ma[1], Jin-Ling Jiang[1], Wei-Xiang Qi[2], Jia-Yi Chen[2], Hao-Ping Xu[2]

[1]Department of Oncology; Ruijin Hospital, Shanghai Jiaotong University School of Medicine, Shanghai, 200025, People's Republic of China;
[2]Department of Radiation Oncology, Ruijin Hospital, Shanghai Jiaotong University School of Medicine, Shanghai, 200025, People's Republic of China

Correspondence: Hao-Ping Xu, Email xhp11701@rjh.com.cn

Introduction: Pancreatic cancer is one of the most common malignant tumors and is characterized by high malignancy, occult incidence and poor prognosis. Traditional chemotherapy drugs have limited efficacy and strong side effects. Therefore, there is an urgent need for a better treatment of the malignancy.

Methods: The prepared arginine glycine peptide (RGD)-human serum albumin (HSA)-Gemcitabine (GEM)/Curcumin (CUR) nanoparticles (NPs) were characterized for physicochemical properties, stability and in vitro release. Comparisons of HSA-GEM/CUR NPs and RGD-HSA-GEM/CUR NPs regarding tissue distributions and pharmacodynamics were also carried out using mice as the animal models.

Results: Transmission electron micrographs showed that RGD peptide-conjugated HSA-NPs had an irregular surface, good dispersion (PDI=0.139±0.03) and a uniform size distribution (Mean PS=115.6±5.7 nm). The ζ-potential was −17.3 mV. As regards in vitro release, non RGD modified NPs showed a faster release rate in 24 hours, yielding a release amount of 75% for GEM and 72% for CUR. RGD-HSA-GEM/CUR NPs exhibited 67% of accumulated release of GEM (63% for CUR) in 24 hours. This may be due to the HSA chain covering the surface of NPs, which hindered the drug release. The cytotoxicity of GEM/CUR co-loaded NPs was significantly higher than that of single-drug NPs ($P < 0.05$). In vivo study results indicated that RGD-HSA-GEM/CUR NPs had notable targeting effect on subcutaneous tumors, with a potential to actively deliver drugs to tumor tissues.

Conclusion: In this study, we prepared RGD-HSA-GEM/CUR NPs that had both good water solubility and tumor-targeting property. The results also showed that the RGD modified NPs had advantages in increasing GEM/CUR concentration at tumor sites and reducing its distribution in peripheral organs.

Keywords: arginine glycine peptide, human serum albumin, Gemcitabine/Curcumin, nanoparticles, pancreatic cancer

Introduction

Pancreatic cancer is one of the most common malignant tumors and is characterized by high malignancy, occult incidence and poor prognosis.[1] At present, surgery is the only cure. However, due to the lack of early specific symptoms as well as the cancer's short course and rapid progress, surgery alone cannot produce the desired effect. Most patients with pancreatic cancer receive chemotherapy as the primary treatment,[2] some undergo a combination of radiotherapy and chemotherapy, which is another main clinical treatment of pancreatic cancer. However, most pancreatic cancer cases are either insensitive to chemotherapy or develop resistance against it during the course of treatment, thus greatly reducing the 5-year survival rate of patients.[3,4]

Gemcitabine (GEM) is a commonly used chemotherapy drug for pancreatic cancer that can lead to significant tumor cell apoptosis.[5] With drug resistance of pancreatic cancer cells as an important reason for the failure of chemotherapy,[6] studies have shown that the resistance to gemcitabine may be due to the decrease of drug uptake or the increase of drug efflux caused by resistance-related proteins, or the change of the activity of the cell apoptosis pathway.[7] The main

Received: 18 March 2022
Accepted: 27 June 2022
Published: 26 July 2022

mechanism could be that resistance-related proteins cause the activity change of PI3K, Akt and other signal regulatory transduction pathways.[8,9]

Curcumin (CUR) is a natural fatty acid synthase inhibitor. Studies have shown that curcumin can inhibit the proliferation of many kinds of cancer cells that play an important role in the occurrence and development of tumor,[10] and facilitate their apoptosis. The mechanism of curcumin mainly operates through affecting the lipid metabolism of tumor cells, reducing the synthesis of intracellular fatty acids, and then inhibiting tumor cell proliferation.[11] At the same time, curcumin regulates a variety of protein molecular pathways in cells, and induces cell apoptosis.[12] It has been reported that curcumin can play an anti-tumor role in the treatment of breast cancer, lung cancer, cervical cancer, ovarian cancer, pancreatic cancer, etc.[13–15]

Nab-paclitaxel is a new paclitaxel preparation with albumin as a drug carrier to avoid the toxic effect of the cosolvent containing Cremophor EL in traditional paclitaxel preparation.[16,17] In addition, with the assistance of albumin, drugs can accumulate more effectively in tumor tissues. Compared with traditional paclitaxel, nab-paclitaxel has higher concentration in tumors and stronger anti-tumor effect.[18,19]

Some studies have shown that nab-paclitaxel can bind to SPARC protein in tumor stroma and stay in tumor tissue to form higher local drug concentration.[20] It may also inhibit the growth of tumor stromal cells and reduce the interstitial tissue of pancreatic cancer, which is conducive to the arrival and action of chemotherapy drugs on tumor cells.[21] The biological characteristic of pancreatic cancer to involve more stromal tissues and less blood vessels is considered to be an important mechanism for its chemotherapy resistance. The tumor stroma inhibiting effect can be further expanded when the albumin carrier platform is combined with other chemotherapeutic drugs, leading to important breakthroughs in the chemotherapy of pancreatic cancer.[22,23] Therefore, in this study, we intended to use an albumin preparation platform to encapsulate GEM and CUR at the same time, in order to obtain more desirable results in pancreatic cancer treatment.

At present, receptor-mediated targeted drug delivery systems are a much sought-after area of research. RGD is a short peptide containing arginine glycine aspartate (Arg-Gly-ASP) as an integrin αvβ3 and its ligand, which mediates the interaction between exogenous and cells. Tumor cells or neovascularization can express some integrins, such as αvβ3.[24,25] It can bind the RGD peptide with a certain affinity and become a new target for tumor therapy. It has been reported that RGD peptide modified liposomes can effectively improve the targeting ability of drug carriers against tumor cells. It can be therefore inferred that an RGD peptide modified albumin platform can enhance the targeting ability of drug carriers against tumor cells and improve drug concentration in tumor tissues.[26,27]

In this study, we prepared RGD-HSA-GEM/CUR NPs that had both good water solubility and tumor-targeting property. The generated NPs were characterized for physicochemical properties, stability and in vitro release. Comparisons of HSA-GEM/CUR NPs and RGD-HSA-GEM/CUR NPs regarding tissue distributions and pharmacodynamics were also carried out using mice as the animal models. The main purpose of this study was to examine whether the combination of two chemotherapeutic drugs could improve tumor targeting and curative effects.

Materials

GEM and CUR were gifted by Yangzijiang Biopharma Co Ltd., (Jiangsu, China). The RGD peptide (MW =1100 Da) was purchased from Biochempartner (Shanghai, China). SW1990 cells cancer cell lines were purchased from the Shanghai Institute of Biochemistry and Cell Biology. The chemical and solvents used were of analytical or HPLC grade. In this study, deionized water was used. Balb/c mice (5–6 weeks old, 22±2 g) were obtained from the Laboratory Animal Center of Faculty at the Shanghai Jiaotong University School of Medicine, China. All animals were free of pathogens and had free access to food and water. Animal experiments were carried out in accordance with the guidelines issued by the National Institutes of Health and approved by the Shanghai Jiaotong University School of Medicine (SYDW20210911).

Preparation of RGD-HSA Loaded GEM/CUR Nanoparticles

The HSA-GEM/CUR NPs were prepared by the emulsion-solvent evaporation method using a high-pressure homogenizer. The initial concentration of HSA was 16 mg/mL in 10 mL deionized water. A mixture of chloroform and ethanol (5 mL) was added to the initial HSA solution at the ratio of 92:8.

GEM (5 mg) and CUR (3 mg) were dissolved in a mixture of chloroform and ethanol (92:8), and then mixed with the HSA solution by volume. This emulsion was first homogenized for 2 minutes before being treated by a hand-held Omni Micro homogenizer, followed by high-pressure homogenization. A homogenization pressure of 15,000 psi was applied to the emulsion, and 10 homogenization cycles were performed. The emulsion subjected to various homogenization cycles was passed through the homogenizer valve and collected through a connecting tube at the base of the assembly to form nano-sized emulsion droplets. After high-pressure homogenization, the obtained colloidal solution was transferred to a round bottom flask, and a vacuum pressure of 400 mm Hg was applied at 40 °C for 30 minutes with rotated evaporation at 75 rpm. This process ensured the complete removal of the organic solvent from the emulsion, resulting in the formation of HSA-GEM/CUR NPs.

To conjugate RGD peptide to HSA-GEM/CUR NPs, HSA-GEM/CUR NPs modification with MBS (Methyl methacrylate-Butadiene-Styrene) was performed as described by Masahiro Tomita.[28] HSA-GEM/CUR NPs were activated for half an hour at room temperature with MBS (10 mg/mL in DMF, heterobifunctional cross-linker). After activation, the suspension and the RGD peptide were co-incubated at room temperature for 3 hours at a molar ratio of 10:1. In this step, the maleimido group of MBS reacted with the free sulfhydryl group of the Cys residue on the peptide. The reaction mixture was then dialyzed against PBS (pH 7.2) at 4°C overnight.

Physicochemical Characterization

A transmission electron microscope, a scanning electron microscope, and a Zetasizer (Nano ZS90; Malvern Instruments Ltd, Worcestershire, UK) were used to analyze the morphology, particle size, and ζ-potential, respectively, of the prepared HSA-GEM/CUR NPs and RGD-HSA-GEM/CUR NPs.

The drug-loading coefficient (DL%) and the encapsulation ratio (ER%) were calculated as follows. Firstly, GEM and CUR were extracted from the NPs with 1 mL 2% acetic acid/acetonitrile (1:1, v/v). The extracted solution was then properly diluted prior to HPLC analysis. The contents of GEM and CUR in the NPs were determined by the HPLC method described below, and DL% and ER% were calculated according to Eq. (1) and Eq. (2):

$$DL\% = WM/(WP + WM) \times 100 \quad (1)$$

$$ER\% = WM/WF \times 100 \quad (2)$$

Where WP is the weight of the initial feeding polymer, WM is the weight of drug incorporated in NPs, and WF is the weight of the initial feeding drug.

Stability

The stability of RGD-HSA-GEM/CUR NPs was examined as follows. The prepared RGD-HSA-GEM/CUR NPs were freeze-dried and stored at room temperature. The average particle size, ζ-potential, PDI, DL% and ER% of the NPs were measured at different time points.

Release Experiments

The amounts of GEM and CUR released from free GEM/CUR, HSA-GEM/CUR NPs and RGD-HSA-GEM/CUR NPs were measured by the dialysis method. The samples (= 10 mg drug, GEM:CUR=5:3) were placed in a dialysis bag (molecular weight cutoff 10,000 Da) and dialyzed against 150 mL of PBS (containing 0.1% Tween 80, pH 7.4) at 37°C with gentle shaking. At predetermined time points, a 2 mL sample was removed and replaced with 2 mL of release medium equilibrated to 37°C ± 0.5°C. The drug content of the withdrawn samples was determined by HPLC.

Cellular Uptake

Using coumarin-6 as a fluorescent probe, the uptake of HSA-GEM/CUR NPs or RGD-HSA-GEM/CUR NPs was observed by a laser confocal fluorescence microscope. In short, 35mm cell culture dishes were seeded with SW1990 cells and adhered to the wall after 24 hours, the cell density of each dish being 5×10^4. The media was then replaced with new serum-free media containing blank NPs, free GEM/CUR, HSA-GEM/CUR NPs or RGD-HSA-GEM/CUR NPs,

respectively (equivalent to 0.1 μg/mL of coumarin-6). After incubated for 2 hours, the cells were washed with PBS and fixed with 4% paraformaldehyde. Finally, a laser confocal fluorescence microscope was used to observe the binding and internalization of the NPs.

For further quantitative analysis, 1×10^5 SW1990 cells were seeded in 12-well plates and cultured with serum-free media containing blank NPs, HSA-GEM/CUR NPs or RGD-HSA-GEM/CUR NPs, respectively (equivalent to 0.1 μg/mL of coumarin-6) for 2 hours. At a predetermined time point, cells were collected and washed with PBS. Then, the cells were resuspended in PBS and analyzed by flow cytometry immediately.

In vitro Cytotoxicity

The cell viability was measured by CCK-8 in the following steps: SW1990 cells in the logarithmic phase were suspended in 96 wells at a density of 5×10^3/mL and incubated overnight. The new media of different concentrations preparations, such as blank NPs, free GEM/CUR, HSA-GEM/CUR NPs and RGD-HSA-GEM/CUR NPs, were used to replace the media and plates were incubated for 24 hours. The CCK-8 method was used to examine the cell viability. The absorbance was measured at λ=490 nm. Measurements were taken using a microplate reader.

Biodistribution and in vivo Imaging Studies

To evaluate the distribution of the modified and non-modified GEM/CUR NPs in the main organs and tumors after administration, a biodistribution study needed to be carried out. For this reason, subcutaneous SW1990 tumors were grown in mice. Once the tumors reached a volume of 100–150 mm^3, they were considered well-established. The treatment groups (Balb/c mice) comprised free GEM/CUR, HSA-GEM/CUR NPs and RGD-HSA-GEM/CUR NPs (n=8), respectively. A single dose of each preparation, equivalent to 10 mg/kg GEM/CUR (GEM:CUR=5:3), was injected into the mice via the tail vein. At 0.5 h, 4 h and 12 h after injection, the animals were sacrificed by cervical dislocation. Their plasma (0.1 mL) and 0.5 g of organs (tumor, heart, liver, spleen, lung and kidney) were removed and flushed with water for three times to remove the remaining blood for HPLC analysis.

Another batch of animals were selected to evaluate the in vivo imaging results. When the animal model was established, 200 μL of fluorescent probe Dir-labeled (1 mg/kg) free GEM/CUR, HSA-GEM/CUR NPs and RGD-HSA-GEM/CUR NPs were injected into the tumor-bearing mice via the tail vein. After anesthesia, the IVIS imaging system was used to collect the whole-body fluorescence images of mice at 12 h. The exposure time was set at 600 ms, and the fluorescence signal was collected at 780 nm.

Tumor Growth Inhibition Study

The purpose of this study was to evaluate the antitumor ability of GEM/CUR NPs in the SW1990 tumor model. With this in mind, we established a subcutaneous SW1990 tumor model in nude mice. Once the tumor grew to a volume of 100 to 150 mm^3, the animals were randomly divided into groups so that the initial mean tumor volume was consistent across all groups. The comparison groups were given blank NPs, free GEM/CUR, HSA-GEM/CUR NPs and RGD-HSA-GEM/CUR NPs. The mice in the treatment group were given 1 mL of each preparation, which was equivalent to 2 mg/kg GEM/CUR (GEM:CUR=5:3), via the tail vein daily for one week, and the tumors were monitored for their growth and measured every third day. Tumor volumes were estimated as $V\ (mm^3) = (\text{length} \times \text{width}^2)/2$. The body weight was monitored throughout the study to detect signs of drug toxicity. When the control tumor reached 1000 mm^3, the study stopped and the mice were sacrificed by drowning.

Western Blot

The SW1990 cells were seeded in 6-well plates at 5×10^5 cells/well, and the drugs (free GEM/CUR, HSA-GEM/CUR NPs and RGD-HSA-GEM/CUR NPs) were added. The final concentration of the drug was converted to GEM/CUR 0.5 μM, and the cells were treated for 24 h. 5×10^6 cells were collected, and centrifuged at 800~1000 rpm for 5 min. The supernatant was discarded, and cells were washed twice with pre-cooled PBS. 1 mL of protein extraction reagent was added to 100 μL of compacted cells (1 μL of protease inhibitor per mL of extractant, 1 μL of DTT, 10 μL of PMSF). The maximum speed of the vortex oscillator was used for 1 min, followed by ice bath for 10~15 min. The oscillation was

conducted 2~3 times for 30 sec each time. Centrifuge was performed at 14,000×g for 15 min at 4 °C, and the supernatant was transferred to a pre-cooled EP tube to obtain total protein. Protein (40 μg) was separated by 10% SDS-PAGE and stained with antibodies, and analyzed using electrochemiluminescence.

Statistics Analysis

Data are expressed as mean ± SD. Student's *t*-test was used for the analysis of differences between any two groups, and multiple groups were analyzed by the one-way analysis of variance test. All statistical analyses were conducted using the SPSS software (version 22.0; IBM Corporation, Armonk, NY, USA). A value of $P < 0.05$ was considered statistically significant.

Results

Preparation and Characterization

In this study, we used a high-pressure homogenizer and the emulsion-solvent evaporation method to prepare RGD-HSA-GEM/CUR NPs. NPs with a smooth surface, good dispersion and relatively uniform size distributions were selected. To modify HSA-NPs with the RGD peptide, HSA-NPs suspension was pre-incubated with MBS. The activated HSA-NPs were then incubated with the RGD peptide. Transmission electron micrographs showed that RGD peptide-conjugated HSA-NPs had an irregular surface, good dispersion (PDI=0.139±0.03) and a uniform size distribution (Mean PS=115.6 ±5.7 nm). The ζ-potential was −17.3 mV. Non-conjugated and conjugated nanoparticles were then observed by TEM (Figure 1A and B). The other parameters are shown in Table 1. The preliminary test results showed that the diameters of the NPs increased in a directly proportional manner with respect to the drug-to-HSA ratio (w/w). However, only a slight difference in particle size was observed between the ratio of 0.1 and 0.2. The DL (%) at the drug-to-HSA ratio of 0.2 was 13.6%, which was much higher than the value of 5.1 wt% observed at the drug-to-HSA ratio of 0.1. No significant difference in the DL was seen at drug-to-HSA ratios ranging from 0.2 to 0.4. Moreover, the highest ER (%) was obtained at the drug-to-HSA ratio of 0.2, which was 82.2 ± 4.5%, much higher than that of other preparations. Therefore, 0.2 was selected as the optimum drug-to-HSA ratio (w/w) for NP synthesis.

Stability

The stability of the RGD-HSA-GEM/CUR NPs was important for storage. In our study, there were no significant differences in the average particle size, ζ-potential, PDI, DL% and ER% at 0, 1, 3 and 6 months ($P > 0.05$) (Table 2). At the same time, the surface morphology showed that the shape of RGD-HSA-GEM/CUR NPs did not change after 6 months (Figure 1C).

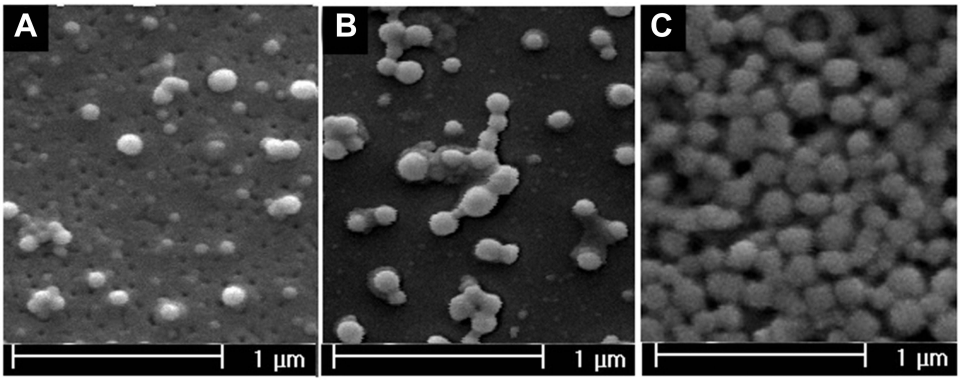

Figure 1 Transmission electron microscope of HSA-GEM/CUR NPs (**A**); RGD-HSA-GEM/CUR NPs (**B**); RGD-HSA-GEM/CUR NPs after 6 months (**C**).

Table 1 The Characteristics of Different Formulations: Particle Size, Entrapment Ratio, Polydispersity Index and ζ-Potential. (Mean ± SD, n=3)

	Particle Size (nm)	Encapsulation Ratio (%)	Polydispersity Index (PDI)	ζ-potential (mV)
HSA-GEM/CUR NPs	113.6±6.1	81.4±5.1	0.131±0.06	−15.9±2.4
RGD-HSA-GEM/CUR NPs	115.6±5.7	82.2±4.5	0.139±0.03	−17.3±1.6

Table 2 Stability Test Observations of the RGD-HSA-GEM/CUR NPs at Room Temperature (Mean ± SD, n=3)

	Time (m)	Physical Changes	Particle Size (nm)	Encapsulation Ratio (%)	Polydispersity Index (PDI)	ζ-potential (mV)
Room temperature	0	-	115.6±5.7	82.2±4.5	0.139±0.03	−17.3±1.6
	1	-	117.3±4.6	81.1±3.7	0.142±0.05	−18.5±1.8
	3	-	118.1±3.9	81.4±2.9	0.147±0.06	−17.9±1.3
	6	-	120.6±6.1	80.2±3.1	0.141±0.04	−18.1±1.4

Note: No physical change.

Release Experiments

The in vitro drug release profiles of free GEM/CUR, HSA-GEM/CUR NPs and RGD-HSA-GEM/CUR NPs, are illustrated in Figure 2. The release of free drug was much faster than that of NPs formulations, which achieved over 90% in 2 hours. Non RGD modified NPs showed a faster release rate in 24 hours, yielding a release amount of 75% for GEM and 72% for CUR. RGD-HSA-GEM/CUR NPs exhibited 67% accumulated release of GEM (63% for CUR) in 24 hours. This may be due to the HSA chain covering the surface of NPs, which hindered the drug release.[29] The main

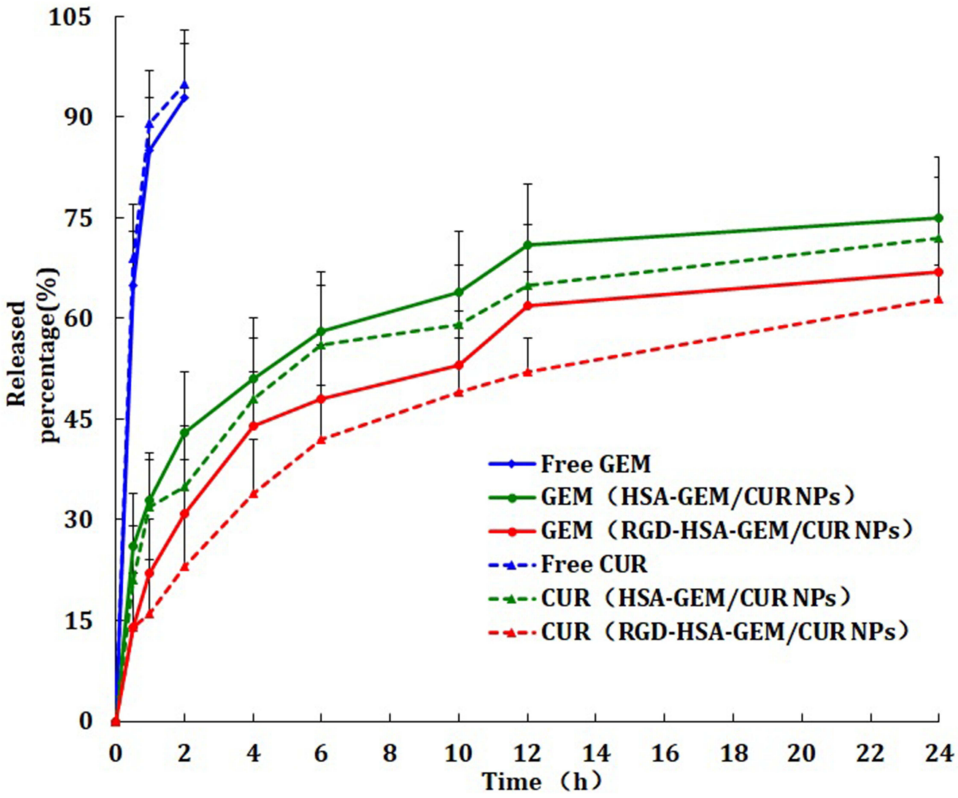

Figure 2 The release profile of drug in NPs in PBS (containing 0.1% Tween 80, pH 7.4) (n=6).

reason for the initial burst release is that the drug on the surface of NPs was released into the medium first and then into the core of NPs. Since the modification of RGD did not affect the spatial structure of NPs, there was no significant difference in the release curves between modified and non-modified NPs.

Cellular Uptake

The cellular uptake was estimated in SW1990 cells by fluorescence measurement using coumarin-6 as a fluorescent probe. Figure 3A–D show fluorescence microscopy images of different sample groups. The fluorescence intensity of free GEM/CUR was the lowest observed among all formulations. The fluorescence intensity of the RGD modified group was a little stronger than that of the non-RGD modified group, which was proposed to be related to the targeting capacity of the αvβ3 integrin. Results showed that depending on surface modification could indicate when cell internalization was changed and more drugs entered the cells successfully. In the quantitative cell uptake study, coumarin-6 in the three formulations was quantified by recovering drug NPs from cells and measuring their fluorescence (normalized to per mg of the total cellular protein contents). The quantitative analysis produced results extremely similar to those obtained from the fluorescence imaging. As shown by Figure 3E, there were significant differences in fluorescence intensity among the RGD modified groups.

In vitro Cytotoxicity

Good biocompatibility is a primary concern for the design of drug delivery systems. To evaluate the biocompatibility of NPs in vitro, SW1990 cells were mixed with different concentrations preparations of NPs (blank NPs, free GEM/CUR, HSA-GEM/CUR NPs and RGD-HSA-GEM/CUR NPs), respectively (Figure 4). All drug loaded samples inhibited the growth of tumor cells. With the increase of drug concentration, the inhibitory effect was also enhanced. The IC50 values of GEM and CUR on different samples are summarized in Table 3. The cytotoxicity of GEM/CUR co-loaded NPs was significantly higher than that of single-drug NPs ($P < 0.05$). RGD-HSA-GEM/CUR NPs had the highest cytotoxicity ($P < 0.05$).

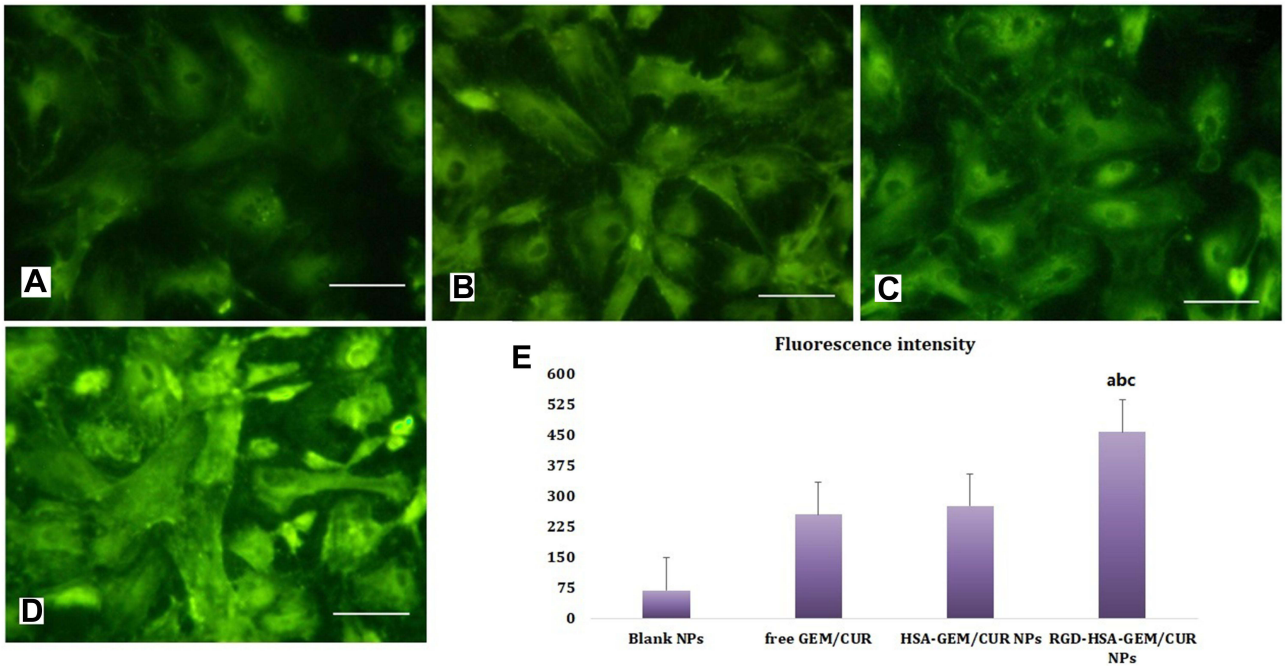

Figure 3 Confocal images of cellular uptake of Blank NPs (**A**); free GEM/CUR (**B**), HSA-GEM/CUR NPs (**C**) and RGD-HSA-GEM/CUR NPs (**D**) by SW1990 cells. Incubation time was 2 hours. (**E**) was the quantitative results. Bar=50 μm. ($^{a}p < 0.05$, RGD-HSA-GEM/CUR NPs vs Blank NPs; $^{b}p < 0.05$, RGD-HSA-GEM/CUR NPs vs free GEM/CUR, $^{c}p < 0.05$, RGD-HSA-GEM/CUR NPs vs HSA-GEM/CUR NPs).

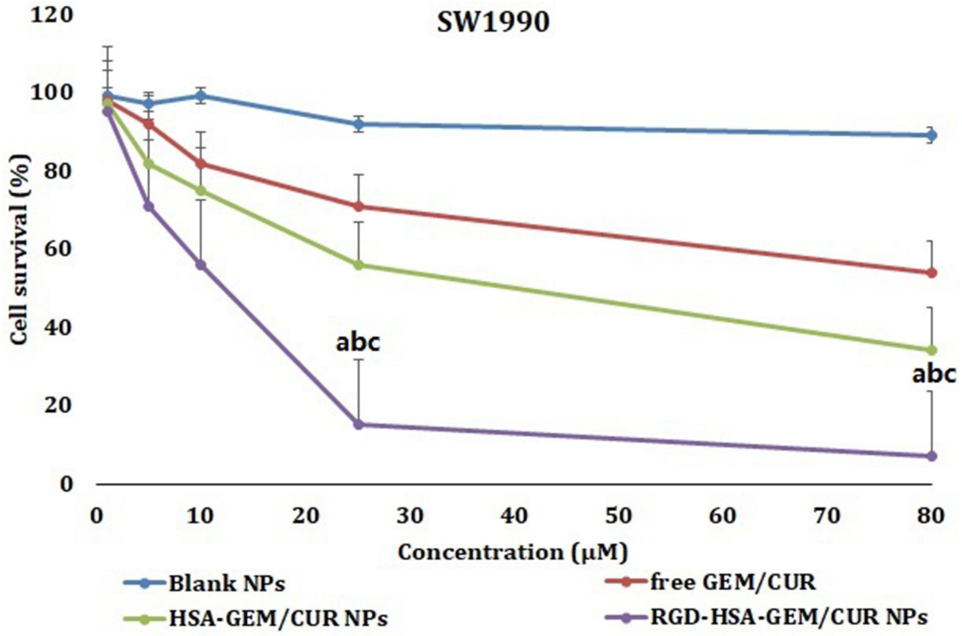

Figure 4 In vitro viability of different NPs formulations in SW1990 cells. Data represents mean ± SD (n = 3). A Cell viability cultured with Blank NPs; free GEM/CUR, HSA-GEM/CUR NPs and RGD-HSA-GEM/CUR NPs at various concentrations of GEM/CUR after 24 h. (^{a}p <0.05, RGD-HSA-GEM/CUR NPs vs Blank NPs; ^{b}p <0.05, RGD-HSA-GEM/CUR NPs vs free GEM/CUR, ^{c}p <0.05, RGD-HSA-GEM/CUR NPs vs HSA-GEM/CUR NPs).

Biodistribution and in vivo Imaging Studies

A biodistribution study was performed to investigate the distribution of modified and non-modified GEM/CUR NPs in vivo. As shown in Figure 5A–G, in the group of free GEM/CUR, plasma drug concentration peaked at 0.5h and was then rapidly eliminated with no selective accumulation in any tissue. In both free GEM/CUR and HAS-GEM/CUR NPs, the distribution of drug in vivo was relatively balanced and there was no obvious organ accumulation (Figure 5). The levels of GEM/CUR distribution in tumor were limited in two groups. As for the RGD-HSA-GEM/CUR NPs group, the distribution of drug in different tissues varied significantly. It accumulated in higher quantities in tumors compared to the other treatment groups. The GEM/CUR concentration in mice tumor (GEM 678 ng/g, CUR65412hrs) in the RGD-HSA-GEM/CUR NPs group was significantly higher than that in other tissues and the plasma (Figure 5A). GEM/CUR showed the highest value of AUC_{0-t} and Target index (TI) in tumor, and the difference was statistically significant ($p<0.05$). The TI of different formulations are listed in Table 4. This phenomenon of tumor enrichment may be attributable to the receptor-mediated mechanism, which could bring benefits to clinical treatment. Meanwhile, Figure 6 shows that after being given near infrared probe Dir 12h and examined by organ imager, RGD-HSA-GEM/CUR NPs had stronger fluorescence in the nude mouse's subcutaneous tumor site than other groups. This indicated that RGD-HSA-GEM/CUR

Table 3 The IC50 Values of Free Gemcitabine/Curcumin (GEM/CUR), Human Serum Albumin-Gemcitabine/Curcumin Nanoparticles (HSA-GEM/CUR NPs) and Arginine Glycine Peptide-Human Serum Albumin-Gemcitabine/Curcumin Nanoparticles (RGD-HSA-GEM/CUR NPs) Treated SW1990 Cells (Mean ± SD, n=6)

Formulations	SW1990 IC50 (μM)
Free GEM/CUR	51.2±3.24*
HSA-GEM/CUR NPs	18.3±2.33*
RGD-HSA-GEM/CUR NPs	11.1±1.13

Note: *p<0.05 vs the group of RGD-HSA-GEM/CUR NPs.

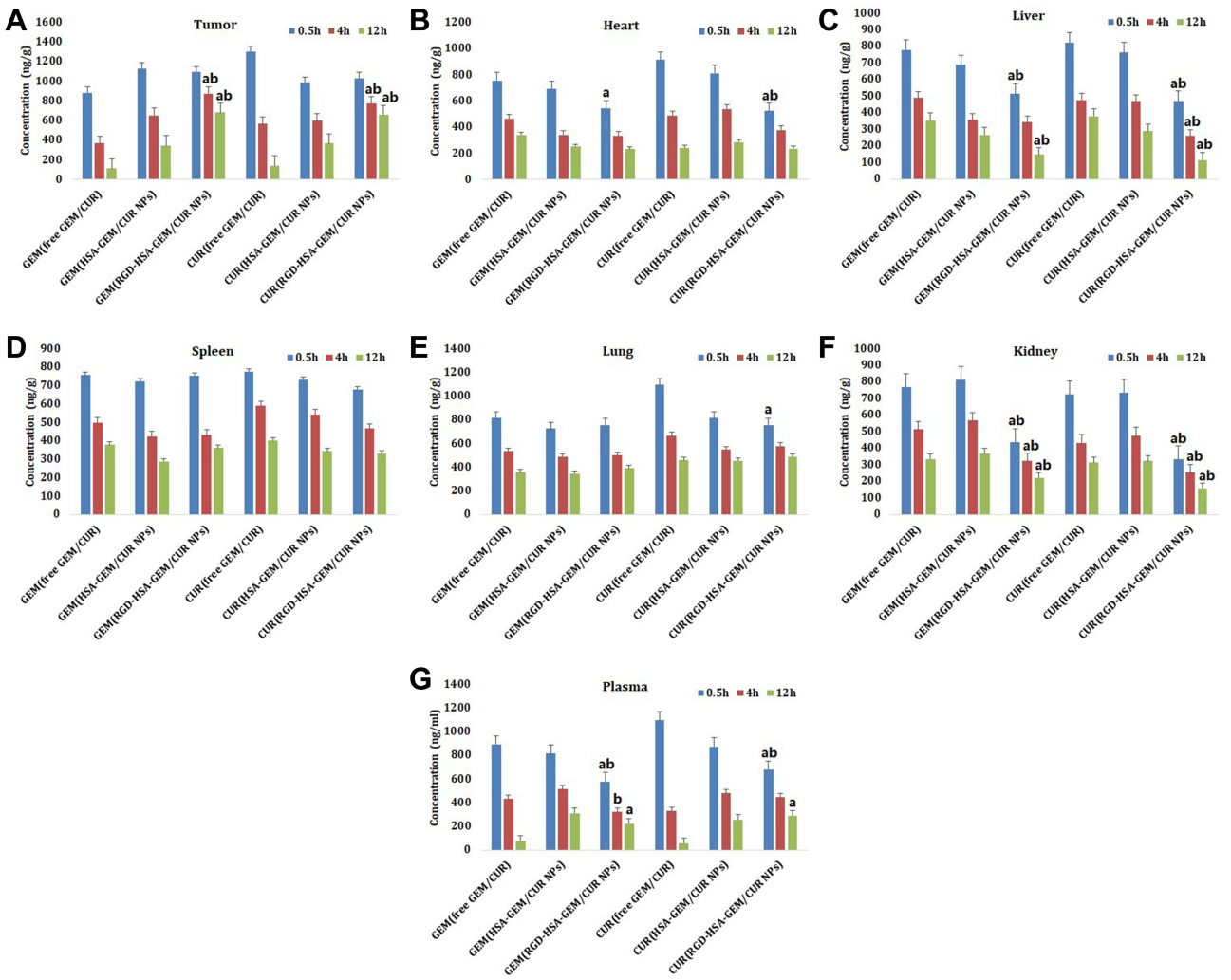

Figure 5 In vivo biodistribution study of modified and non-modified GEM/CUR NPs (n=8). (**A**) tumor, (**B**) heart, (**C**) liver, (**D**) spleen, (**E**) lung, (**F**)kidney and (**G**) plasma. ([a]p <0.05, RGD-HSA-GEM/CUR NPs vs free GEM/CUR, [b]p <0.05, RGD-HSA-GEM/CUR NPs vs HSA-GEM/CUR NPs).

NPs had notable targeting effect on subcutaneous tumors, with a potential to actively deliver drugs to tumor tissues. This result also showed that the RGD modified NPs had advantages in increasing GEM/CUR concentration at tumor sites and reducing its distribution in peripheral organs.

Tumor Inhibition Study

Through the tumor growth inhibition experiment, the therapeutic effect of different GEM/CUR NPs in vivo was evaluated. Compared with the control group and the free GEM/CUR treatment group, all GEM/CUR NPs groups showed inhibited tumor growth at the experimental dose. RGD-HSA-GEM/CUR NPs were most effective in controlling tumor growth throughout the 27-day study (Figure 7A). The growth trends of the three groups were similar at the beginning of the study but changed halfway through. From day 15, there was a significant difference in tumor volume between free GEM/CUR, HSA-GEM/CUR NPs and RGD-HSA-GEM/CUR NPs groups. At the end of the study, the tumor volumes were 781.4 ± 67.5 mm^3 for the control group, 687.3 ± 59.4 mm^3 for the free GEM/CUR group, 545.7 ± 57.2 mm^3 for the HSA-GEM/CUR NPs group, and 354.6 ± 39.8 mm^3 for the RGD-HSA-GEM/CUR NPs group. The RGD-HSA-GEM/CUR NPs treatment was consistently more effective in controlling tumor growth than other treatments throughout the study. The mouse weights recorded throughout the study were fairly constant, indicating that the preparation was not significantly toxic (Figure 7B).

Table 4 The Mean AUC_{0-t} and Target Index of Different Formulations of NPs in Different Organs of Mice (Mean ± SD, n=8)

AUC_{0-t} (ngh/g)	GEM(Free GEM/CUR)	GEM(HSA-GEM/CUR NPs)	GEM(RGD-HSA-GEM/CUR NPs)	CUR(Free GEM/CUR)	CUR(HSA-GEM/CUR NPs)	CUR(RGD-HSA-GEM/CUR NPs)
Tumor	4096.5±327.2	7096.8±540.9	9637.0±656.3	6055.0±398.5	6617.0±412.3	8832.8±433.6
Heart	5364.8±298.3	4188.3±329.7	3791.3±327.5	5379.8±376.3	5662.5±309.2	4032.8±309.2
Liver	5201.5±343.2	2871.6±293.4	2653.9±253.2	5629.4±329.1	5410.7±314.3	2432.6±298.3
Spleen	5688.8±432.1	4845.5±378.5	5239.5±367.5	6340.8±436.4	5775.3±331.3	5172.3±287.5
Lung	5901.8±309.2	5445.5±438.6	5739.0±219.4	7564.5±459.4	6376.5±378.4	6583.0±423.5
Kidney	5624.0±312.5	6141.3±548.7	3487.5±328.1	4995.5±321.4	5305.5±298.7	2673.5±278.3
Plasma	4351.3±298.3	5609.0±438.6	3741.3±287.5	4029.0±309.2	5279.0±310.2	4901.3±309.2
TI(Tumor/Heart)	0.76	1.69	2.54[ab]	1.13	1.17	2.19[cd]
TI(Tumor/Liver)	0.79	2.47	3.63[ab]	1.08	1.22	3.63[cd]
TI(Tumor/Spleen)	0.72	1.46	1.84[a]	0.95	1.15	1.71[cd]
TI(Tumor/Lung)	0.69	1.30	1.68[a]	0.80	1.04	1.34[c]
TI(Tumor/Kidney)	0.73	1.16	2.76[ab]	1.21	1.25	3.30[cd]
TI(Tumor/Plasma)	0.94	1.27	2.58[ab]	1.50	1.25	1.80[d]

Notes: [a]p<0.05: GEM(RGD-HSA-GEM/CUR NPs) vs GEM(free GEM/CUR); [b]p<0.05: GEM(RGD-HSA-GEM/CUR NPs) vs GEM(HSA-GEM/CUR NPs); [c]p<0.05: CUR(RGD-HSA-GEM/CUR NPs) vs CUR(free GEM/CUR); [d]p<0.05: CUR(RGD-HSA-GEM/CUR NPs) vs CUR(HSA-GEM/CUR NPs).

Western Blot

To further analyze the mechanism of enhanced apoptosis seen in the nano drug-loading system, we again treated SW1990 cells with the same dose (GEM/CUR 0.5 μM) of free GEM/CUR, HSA-GEM/CUR NPs and RGD-HSA-GEM/CUR NPs. Flow cytometry analysis showed that this concentration was sufficient to promote apoptosis after 24 hours, and the expression of apoptotic proteins in each drug group for 24 h was evaluated using the Western Blot. The results and analysis are shown in Figure 8A and B. The results revealed that the expression of the anti-apoptotic protein Bcl-2 in drug-treated cells was downregulated when modified with RGD. By contrast, the pro-apoptosis proteins Bax, caspase-3 and caspase-9 demonstrated a notable increase in protein expression following treatment with RGD-HSA-GEM/CUR NPs compared with the other groups ($P < 0.05$). The data indicated that the strategy with RGD modified increased the inhibitory effect of GEM/CUR on the viability of SW1990 cells, potentially by stimulating apoptosis, which may be mediated by the modulation of Bax, Bcl-2, caspase-3 and caspase-9 apoptotic factors.

Conclusions

In this study, RGD modified HSA-GEM/CUR NPs drug carriers were constructed. The NPs prepared were of a uniform size, a smooth surface and a spherical shape, and were dispersed evenly. The in vitro release profiles indicated a sustained release of GEM/CUR from the NPs. The results of biodistribution and pharmacodynamics studies both showed that the

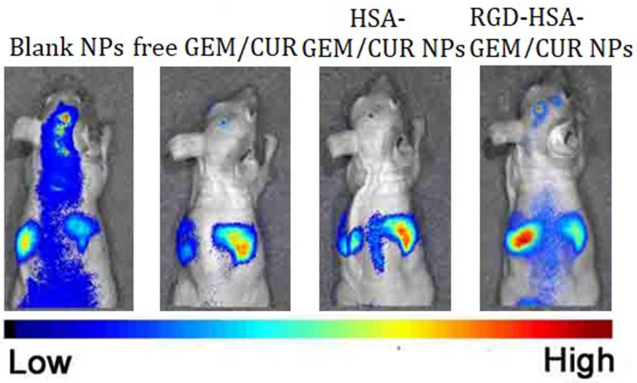

Figure 6 The in vivo imaging of DiR-loaded Blank NPs; free GEM/CUR, HSA-GEM/CUR NPs and RGD-HSA-GEM/CUR NPs in tumor bearing nude mice at 12 h (n=3).

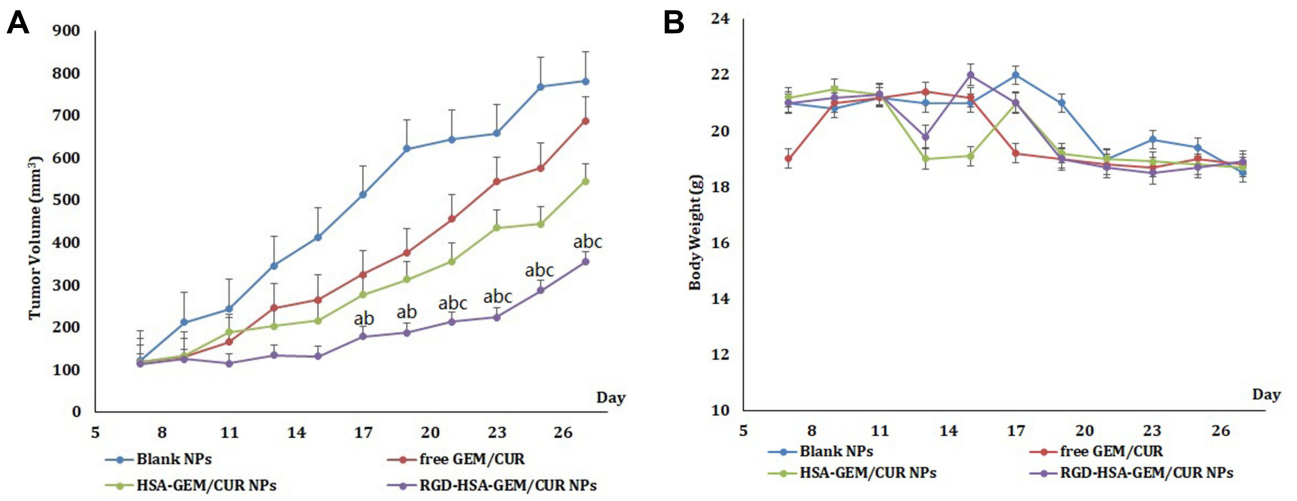

Figure 7 (**A**) The growth curves of SW1990 tumors in mice. (**B**) The changes in the body weight of SW1990 tumor-bearing mice. ([a]p <0.05, RGD-HSA-GEM/CUR NPs vs Blank NPs; [b]p <0.05, RGD-HSA-GEM/CUR NPs vs free GEM/CUR, [c]p <0.05, RGD-HSA-GEM/CUR NPs vs HSA-GEM/CUR NPs).

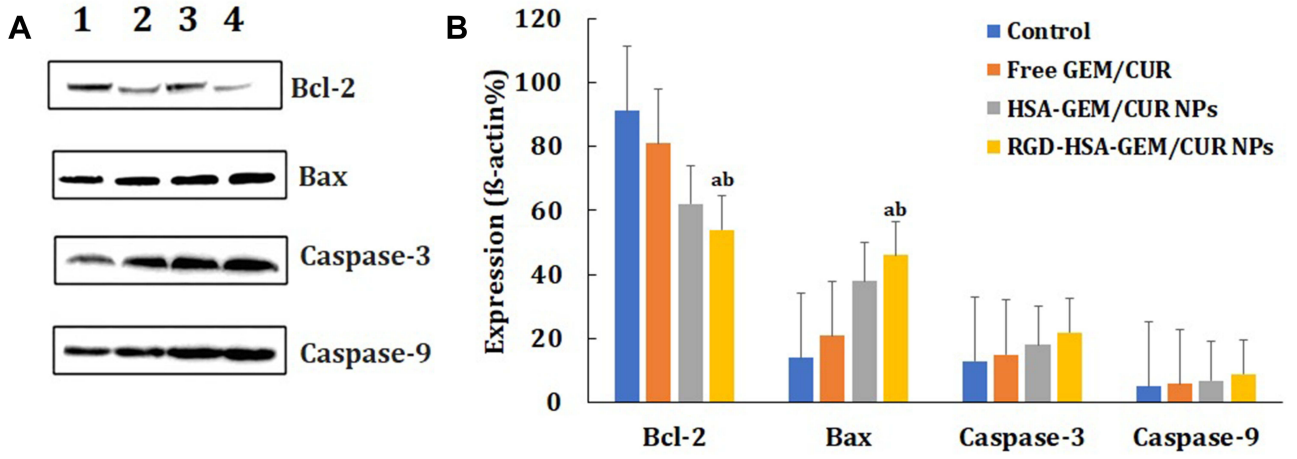

Figure 8 Analysis of apoptotic pathway proteins. Western Blot result of apoptotic protein expression (**A**) and expression of actin (**B**) on SW1990 cells after incubated with free GEM/CUR, HSA-GEM/CUR NPs and RGD-HSA-GEM/CUR NPs for 24 h (GEM/CUR 0.5 μM). ([a]p <0.05, RGD-HSA-GEM/CUR NPs vs Control; [b]p <0.05, RGD-HSA-GEM/CUR NPs vs free GEM/CUR).

higher effectiveness of RGD-HSA-GEM/CUR NPs could be explained by the fact that RGD modification resulted in a higher cellular uptake of GEM/CUR, which could have increased absorption and provided a higher bioavailability.

Acknowledgment

Thank you very much for Prof Chen Wei of School of pharmacy, Fudan University guidance and help in this study.

Disclosure

The authors report no conflicts of interest in this work.

References

1. Ilic M, Ilic I. Epidemiology of pancreatic cancer. *World J Gastroenterol*. 2016;22(44):9694–9705. doi:10.3748/wjg.v22.i44.9694
2. Goral V.Pancreatic cancer: pathogenesis and diagnosis. *Asian Pac J Cancer Prev*. 2015;16(14):5619–5624. doi:10.7314/APJCP.2015.16.14.5619
3. Chu LC, Goggins MG, Fishman EK. Diagnosis and detection of pancreatic cancer. *Cancer J*. 2017;23(6):333–342. doi:10.1097/PPO.0000000000000290

4. Tempero MA. NCCN guidelines updates: pancreatic cancer. *J Natl Compr Canc Netw*. 2019;17(5.5):603–605. doi:10.6004/jnccn.2019.5007
5. Sarvepalli D, Rashid MU, Rahman AU, et al. Gemcitabine: a review of chemoresistance in pancreatic cancer. *Crit Rev Oncog*. 2019;24(2):199–212. doi:10.1615/CritRevOncog.2019031641
6. Zeng S, Pöttler M, Lan B, Grützmann R, Pilarsky C, Yang H. Chemoresistance in pancreatic cancer. *Int J Mol Sci*. 2019;20(18):4504. doi:10.3390/ijms20184504
7. Ducreux M, Seufferlein T, Van Laethem JL, et al. Systemic treatment of pancreatic cancer revisited. *Semin Oncol*. 2019;46(1):28–38. doi:10.1053/j.seminoncol.2018.12.003
8. Wang Y, Kuramitsu Y, Baron B, et al. PI3K inhibitor LY294002, as opposed to wortmannin, enhances AKT phosphorylation in gemcitabine-resistant pancreatic cancer cells. *Int J Oncol*. 2017;50(2):606–612. doi:10.3892/ijo.2016.3804
9. Ebrahimi S, Hosseini M, Shahidsales S, et al. Targeting the Akt/PI3K signaling pathway as a potential therapeutic strategy for the treatment of pancreatic cancer. *Curr Med Chem*. 2017;24(13):1321–1331. doi:10.2174/0929867324666170206142658
10. Nelson KM, Dahlin JL, Bisson J, Graham J, Pauli GF, Walters MA. The essential medicinal chemistry of curcumin. *J Med Chem*. 2017;60(5):1620–1637. doi:10.1021/acs.jmedchem.6b00975
11. Kotha RR, Luthria DL. Curcumin: biological, pharmaceutical, nutraceutical, and analytical aspects. *Molecules*. 2019;24(16):2930. doi:10.3390/molecules24162930
12. Pescosolido N, Giannotti R, Plateroti AM, Pascarella A, Nebbioso M. Curcumin: therapeutical potential in ophthalmology. *Planta Med*. 2014;80(4):249–254. doi:10.1055/s-0033-1351074
13. Moghadamtousi SZ, Kadir HA, Hassandarvish P, Tajik H, Abubakar S, Zandi K. A review on antibacterial, antiviral, and antifungal activity of curcumin. *Biomed Res Int*. 2014;2014:186864. doi:10.1155/2014/186864
14. Giordano A, Tommonaro G. Curcumin and Cancer. *Nutrients*. 2019;11(10):2376. doi:10.3390/nu11102376
15. Unlu A, Nayir E, Dogukan Kalenderoglu M, Kirca O, Ozdogan M. Curcumin (Turmeric) and cancer. *J BUON*. 2016;21(5):1050–1060.
16. Gradishar WJ. Albumin-bound paclitaxel: a next-generation taxane. *Expert Opin Pharmacother*. 2006;7(8):1041–1053. doi:10.1517/14656566.7.8.1041
17. Von Hoff DD, Ervin T, Arena FP, et al. Increased survival in pancreatic cancer with nab-paclitaxel plus gemcitabine. *N Engl J Med*. 2013;369(18):1691–1703. doi:10.1056/NEJMoa1304369
18. Yardley DA. nab-Paclitaxel mechanisms of action and delivery. *J Control Release*. 2013;170(3):365–372. doi:10.1016/j.jconrel.2013.05.041
19. Kundranda MN, Niu J. Albumin-bound paclitaxel in solid tumors: clinical development and future directions. *Drug Des Devel Ther*. 2015;9:3767–3777. doi:10.2147/DDDT.S88023
20. Kim H, Samuel S, Lopez-Casas P, et al. SPARC-independent delivery of Nab-Paclitaxel without depleting tumor stroma in patient-derived pancreatic cancer Xenografts. *Mol Cancer Ther*. 2016;15(4):680–688. doi:10.1158/1535-7163.MCT-15-0764
21. Cullis J, Siolas D, Avanzi A, Barui S, Maitra A, Bar-Sagi D. Macropinocytosis of Nab-paclitaxel drives macrophage activation in pancreatic cancer. *Cancer Immunol Res*. 2017;5(3):182–190. doi:10.1158/2326-6066.CIR-16-0125
22. Giordano G, Pancione M, Olivieri N, et al. Nano albumin bound-paclitaxel in pancreatic cancer: current evidences and future directions. *World J Gastroenterol*. 2017;23(32):5875–5886. doi:10.3748/wjg.v23.i32.5875
23. Neesse A, Michl P, Tuveson DA, Ellenrieder V. nab-Paclitaxel: novel clinical and experimental evidence in pancreatic cancer. *Z Gastroenterol*. 2014;52(4):360–366. doi:10.1055/s-0034-1366002
24. Tang Z, Feng W, Yang Y, Wang Q. Gemcitabine-loaded RGD modified liposome for ovarian cancer: preparation, characterization and pharmacodynamic studies. *Drug Des Devel Ther*. 2019;13:3281–3290. doi:10.2147/DDDT.S211168
25. Zhu R, Tian Y. Preparation and evaluation of RGD and TAT co-modified docetaxel-loaded liposome. *Drug Des Devel Ther*. 2017;11:3481–3489. doi:10.2147/DDDT.S149620
26. Zhou X, Liu HY, Zhao H, Wang T. RGD-modified nanoliposomes containing quercetin for lung cancer targeted treatment. *Onco Targets Ther*. 2018;11:5397–5405. doi:10.2147/OTT.S169555
27. Cai W, Geng C, Jiang L, et al. Encapsulation of gemcitabine in RGD-modified nanoliposomes improves breast cancer inhibitory activity. *Pharm Dev Technol*. 2020;25(5):640–648. doi:10.1080/10837450.2020.1727920
28. Tomita M, Sugi H, Ozawa K, Tsong TY, Yoshimura T. Targeting antigen-specific receptors on B lymphocytes to generate high yields of specific monoclonal antibodies directed against biologically active lower antigenic peptides within presenilin 1. *J Immunol Methods*. 2001;251(1–2):31–43. doi:10.1016/S0022-1759(01)00299-X
29. Yuan L, Cao Y, Luo Q, et al. Pullulan-Based nanoparticle-HSA complex formation and drug release influenced by surface charge. *Nanoscale Res Lett*. 2018;13(1):317. doi:10.1186/s11671-018-2729-5